

Original Research

RANBP1 Regulates NOTCH3-Mediated Autophagy in High Glucose-Induced Vascular Smooth Muscle Cells

Zhong-jiao Xu^{1,†}, Jian Xu^{1,†}, Wen-jing Lei¹, Xiang Wang¹, Qi-lin Zou¹, Lin-chun Lv¹, Chong Liu¹, Wu-ming Hu¹, Yi-jia Xiang¹, Jia-yi Shen¹, Tie-min Wei^{1,*}, Chun-lai Zeng^{1,*}

Submitted: 5 October 2024 Revised: 29 November 2024 Accepted: 16 December 2024 Published: 17 February 2025

Abstract

Background: Vascular smooth muscle cells(VSMCs) phenotypic switching under hyperglycemic conditions accelerates atherosclerotic progression. Notch receptor 3(NOTCH3), a critical stabilizer of VSMC homeostasis implicated in cerebral autosomal dominant arteriopathy with subcortical infarcts and leukoencephalopathy (CADASIL) pathogenesis, ensures vascular integrity; however, its interplay with RAN Binding Protein 1(RANBP1) during pathological hyperglycemia remains uncharacterized. We hypothesize that hyperglycemiainduced autophagic dysregulation is mechanistically governed by the Notch receptor 3 (NOTCH3)/RANBP1 axis, proliferative capacity, and apoptotic signaling in high glucose (HG)-stimulated VSMCs. The aim of this study was to elucidate the regulatory mechanisms of autophagy in VSMCs under HG conditions, with a focus on the NOTCH3/RANBP1 axis and its implications for vascular health. Methods: Bioinformatics analysis was performed on NOTCH3 sequencing data, including weighted gene co-expression network analysis (WGCNA), screening of differentially expressed genes (DEGs), and construction of a protein-protein interaction (PPI) network, to identify the key gene, RANBP1. In vitro experiments, including cell counting kit-8 (CCK-8) assays, quantitative real-time polymerase chain reaction (qRT-PCR), Western blotting (WB), and flow cytometry, were conducted to examine the effects of NOTCH3 knockdown combined with RANBP1 overexpression on glucose-induced autophagy marker expression and cell viability in VSMCs. Results: NOTCH3 knockdown suppressed VSMC proliferation and induced apoptosis, and the cell cycle was stopped at the S phase. Analysis of VSMC sequencing data revealed 38 overlapping genes between the turquoise module and DEGs, 11 (HPF1, RANBP1, CRNKL1, LGALS3, RDX, ECM1, CXCL5, PA2G4, CENPS, ZNF830, and HIST1H4L) of which were significantly underexpressed in VSMC samples with si-NOTCH3. In a dose-dependent manner, HG therapy altered the expression of autophagy-related markers, upregulated NOTCH3, and downregulated phosphorylated mammalian target of rapamycin (p-mTOR). Downregulation of NOTCH3 aggravated the effects of HG on cell viability and autophagy, whereas overexpression of RANBP1 reversed these effects, suggesting an offsetting effect on HG-induced autophagy. Conclusion: On the basis of sequencing technology, bioinformatics analysis and cell experiments, we conclude that the RANBP1/NOTCH3 axis is essential for the control of autophagy and survival of VSMCs under hyperglycemic stress and could provide new insight for the clinical treatment of VSMC-related diseases.

Keywords: RANBP1; NOTCH3; vascular smooth muscle cells; high glucose; autophagy

1. Introduction

Vascular smooth muscle cells (VSMCs) are central to the pathogenesis of a myriad of cardiovascular and cerebrovascular disorders, underpinned by their crucial roles in modulating vascular tone and facilitating vascular remodeling [1,2]. These processes are foundational to the pathophysiology of conditions such as atherosclerosis, hypertension, and stroke [3,4]. VSMCs maintain vascular homeostasis through complex processes, including contraction, migration, proliferation, and secretion of extracellular matrix components [3]. Dysregulation of these cellular functions often leads to the evolution and progression of vascular pathologies. Understanding the molecular mechanisms underlying VSMC behavior holds immense clinical importance, as it provides insights into disease etiology and offers potential therapeutic targets for intervention.

The Notch gene family is widely expressed in animal cells and plays important regulatory roles in the growth, development and apoptosis of various tissues and organs [5,6]. Notch receptor 3 (Notch3) is expressed mainly in human arterial vascular smooth muscle cells. The autoregulatory function of the brain in Notch3 knockout mice is impaired. A Related study has shown that Notch3 mutation can lead to autosomal dominant subcortical infarcts and leukoencephalopathy (CADASIL) [7]. Morrow et al. [8] proposed that the Notch3 signaling pathway is a new important regulator of phenotypic transition in VSMCs. Notch3 plays a special role in the signal transduction mechanism in vascular smooth muscle cells. Notch3 can participate in the expression of mature VSMCs, and its signaling system is involved in angiogenesis and vascular remodeling as well as the differentiation and phenotypic regulation of VSMCs

¹Department of Cardiology, The Fifth Affiliated Hospital of Wenzhou Medical University, Lishui Central Hospital, 323000 Lishui, Zhejiang, China

^{*}Correspondence: lswtm@sina.com (Tie-min Wei); lszengchunlai@mail.zju.edu.cn (Chun-lai Zeng)

[†]These authors contributed equally. Academic Editor: Rajesh Katare

[9,10]; thus, it plays an important role in maintaining the phenotypic stability of VSMCs [6,11]. Understanding the complexity of NOTCH signaling can provide insights into cardiovascular and cerebrovascular disease processes and potential therapeutic targets for medical intervention.

VSMCs play a pivotal role in the pathogenesis of cardiovascular diseases, and their behavior is significantly influenced by the glucose environment. Under high glucose (HG) conditions, VSMCs undergo profound changes, including the activation of autophagy, a cellular process crucial for maintaining homeostasis by degrading and recycling damaged components [12,13]. The regulation of autophagy in VSMCs by HG is complex and involves the interplay of various signaling pathways, such as the mTOR pathway, which is known to be suppressed by HG, thereby inhibiting autophagy in VSMCs [14]. RAN binding protein 1 (RANBP1) is integral to the regulation of the cell cycle, particularly in the control of mitotic spindle assembly and chromosome segregation [15]. The protein's function in nucleocytoplasmic transport is highlighted by its ability to bind to Ran GTPase, facilitating the exchange of GDP for GTP and thereby influencing the nuclear import and export of various proteins [16]. This role is particularly important during cell division, where the precise control of protein localization is paramount for accurate segregation of genetic material. Additionally, the NOTCH signaling pathway, particularly NOTCH3, has been implicated in the regulation of VSMC phenotype and function [17], and its interaction with RANBP1 under HG-induced stress is of particular interest because of its potential roles in nuclear transport and cell cycle control [18,19]. Our study aimed to elucidate the regulatory mechanisms of autophagy in VSMCs under HG conditions with a focus on the NOTCH3/RANBP1 axis and its implications for vascular health.

Given the established role of VSMCs in cardiovascular pathophysiology and the key involvement of the NOTCH signaling pathway in vascular biology, this study aimed to gain a deeper understanding of the molecular interactions that control these processes. NOTCH3 is a receptor in the NOTCH signaling pathway and is involved in vascular homeostasis and pathology. However, the impact of its interaction with RANBP1, a gene involved in nuclear transport and cell cycle control, under stressful conditions such as hyperglycemia, remains poorly understood. We hypothesized that glucose-induced autophagy is directly mediated by the RANBP1-NOTCH3 interaction, which remains poorly understood under stressful conditions such as hyperglycemia. Therefore, analyzing the regulatory effects of NOTCH3 and RANBP1 on autophagy pathways, proliferation, and apoptosis in VSMCs under HG-induced stress will provide a more comprehensive understanding of cellular responses under pathological glucose conditions.

2. Materials and Methods

2.1 Gene Coexpression Network of Sequencing Analysis

We tested the sequencing data quality of 9 groups of VSMC data provided by sequencing institutions, including 3 groups of si-NOTCH3-1, 3 groups of si-NOTCH3-2, and 3 groups of normal controls (NCs), in which NOTCH3 was knocked down by different small interfering RNAs (siR-NAs). Next, weighted gene coexpression network analysis (WGCNA) was carried out on all genes in these samples via the "WGCNA" package (version 1.61) of R software (Peter Langfelder and Steve Horvath, Los Angeles, CA, USA). The optimal soft threshold power was determined to be 8, which meets the criteria for scale-free networks (scale-free $R^2 > 0.85$). A dynamic tree cutting method was used for module detection, and genes were divided into different modules according to their expression patterns. Hierarchical clustering of genes within modules was performed based on differences in topological overlap matrices (TOMs). The correlations and significance between different modules and 9 groups (6 case groups and 3 control groups) were subsequently analyzed. By determining the p value and related Pearson correlation coefficient, the key modules with the most significant relationships with the sample were selected, and the number of genes present in each module was determined.

2.2 Identification of Overlapping Genes

Through the "limma" package of R software (version 3.6.1, R Foundation for Statistical Computing, Melbourne, Victoria, Australia), we screened upregulated and downregulated differentially expressed genes (DEGs) from 9 sequencing samples, with fold changes (FCs) >1.3 and <0.77 set as p<0.05. The bioinformatics platform (https://www.bioinformatics.com.cn/) was subsequently used to perform gene intersection analysis on the differentially expressed genes (DEGs) and turquoise modules to screen out overlapping genes.

2.3 Analysis of Protein-Protein Interactions (PPIs)

To elucidate potential protein-protein interactions within the overlapping genes, we conducted PPI network analysis via the Search Tool for the Retrieval of Interacting Genes (STRING, https://string-db.org/) database. The resulting PPI network was visualized using the open-source network visualization software platform Cytoscape (https://cytoscape.org/). This visualization allowed for a detailed examination of the interactions among proteins. Statistical significance was assessed for the obtained results, with the significance threshold set at p < 0.05.

2.4 Receiver Operating Characteristic (ROC) Curve Analysis and Expression Analysis

We evaluated the clinical diagnostic significance of these key genes individually by analyzing ROC curves via the "timeROC" tool package in R (http://cran.r-project.org



/web/packages/timeROC). At each threshold, we evaluated the sensitivity and 1-specificity, i.e., the true-positive rate and false-positive rate, to construct a ROC curve. Next, the 95% confidence interval (95% CI) and area under the curve (AUC) were calculated, with a higher AUC suggesting a gene with greater clinical diagnostic significance. Finally, the expression levels of key genes in the NC group and the si-NOTCH3 group were compared and visualized via the "ggplot2" package (version 3.6.3) of R software.

2.5 Cell Culture

VSMCs, PASMCs, HASMCs and HUASMCs were purchased from Ningbo Mingzhou Biotech Co., Ltd. (Ningbo, Zhejiang, China), and incubated in DMEM (Gibco, Shanghai, China) supplemented with 10% FBS (Gibco, Shanghai, China) at 37 °C with 5% CO₂. All cells were tested negative for mycoplasma and carried out by Short Tandem Repeat (STR) analysis.

2.6 Cell Viability and Proliferation Assay

As directed by the manufacturer, the Cell Counting Kit-8 assay (Beyotime Biotechnology, Shanghai, China) was used to assess the viability and proliferation of cells. Transfected cells were seeded on 96-well plates with 10 μL of CCK-8 solution added to the wells at 0 h, 24 h, 48 h, 72 h, 96 h, and 120 h, after which the cells were incubated for 2 hours. The absorbance value (optical density; OD) was detected at 450 nm on a microplate reader (BioTek microplate reader) (BioTek Instruments, Inc.Winooski, VT, USA).

2.7 Cell Apoptosis Assay

The cells were cultured in DMEM (Gibco, Shanghai, China) supplemented with 10% FBS for an additional 48 hours after transfection with a nontargeting control (NC) or siRNA. After the cells were trypsinized, apoptosis was detected via an Annexin V-FITC Apoptosis Detection Kit (BD Biosciences, San Jose, CA, USA). Then, the cells were treated with Annexin V-propidium iodide (PI) at room temperature in the dark after being pelleted, washed with cold PBS, and suspended in cold PBS. The cells were stored on ice in the dark and then subjected to flow cytometric analysis using a FACSCalibur system (BD Biosciences). Cell Quest software (BD Biosciences) was used to evaluate the data.

2.8 Cell Cycle Assay

Cells transfected with NC or siRNA were extracted after 48 hours, fixed with 70% ethanol overnight at -20 °C, and stained with PI (Sigma-Aldrich, Shanghai, China) while incubated with ribonuclease A (Takara Biotechnology, Dalian, China) for 30 minutes at room temperature. The cell cycle distribution was investigated via flow cytometry using a FACSCalibur system (BD Biosciences).

2.9 Cell Treatment and Transfection

After reaching 50-60% confluence, HASMCs and HUASMCs were cultured in DMEM containing various doses of glucose (5.5, 10.5, 15.5, and 25.5 mM; Thermo Fisher Scientific, Waltham, MA, USA). Subsequently, HASMCs and HUASMCs were cultured with 25.5 mM glucose for 0, 3, 6, 12, and 24 h. For transient transfection, HASMCs and HUASMCs were seeded in 24-well plates at a density of 2×10^5 cells per well. RANBP1 was overexpressed via a plasmid carrying the RANBP1 gene synthesized by Invitrogen Company (Shanghai, China), whereas siRNAs specifically targeting NOTCH3 and RANBP1 (si-NOTCH3, si-RANBP1 #1 and si-RANBP1 #2), purchased from Jima Gene Company (Shanghai, China), were used to knock down these genes. Lipofectamine 2000 reagent (Invitrogen, Shanghai, China) was used for transfection according to the manufacturer's instructions. Lipofectamine 2000 was diluted in Opti-MEM (Gibco, Waltham, MA, USA) to prepare the transfection mixture. The plasmid DNA or siRNA was diluted in Opti-MEM. Then, Lipofectamine 2000 was added to the diluted DNA or siRNA and mixed gently. The mixture was incubated at room temperature for 15-30 minutes to allow the formation of DNA-lipid or siRNA-lipid complexes. These complexes were added to the VSMCs, which were subsequently incubated for 4–6 hours at 37 °C with 5% CO₂. The medium was then replaced with complete growth medium, and the mixture was incubated further for 24-48 hours to allow protein expression.

2.10 Quantitative Real-Time Polymerase Chain Reaction (qRT-PCR)

We utilized TRIZOL (Shanghai, China) for total RNA extraction and a reverse transcription kit from Vazyme (Nanjing, China) for cDNA synthesis. ABI 7900HT (SYBR Green Mix, Applied Biosystems Inc., Waltham, MA, USA) was used for quantitative PCR using system from Thermo Scientific. Relative expression was determined via the $2^{-\Delta\Delta Ct}$ method and standardized to that of glyceraldehyde-3-phosphate dehydrogenase (GAPDH) as an internal control. All primers were synthesized by Invitrogen (Shanghai, China). The set of primer sequences is shown in Table 1.

2.11 Western Blotting (WB) Assay

We conducted WB experiments according to previous methods [20]. The primary antibodies used includedanti-NOTCH3 (1:1000, ab300527, Abcam, Cambridge, UK), anti-mTOR (1:1000, ab32028, Abcam, Cambridge, UK), anti-p-mTOR (1:1000, ab109268, Abcam, Cambridge, UK), anti-LC3B (1:2000, ab192890, Abcam, Cambridge, UK), anti-p62 (1:1000, ab207305, Abcam, Cambridge, UK), anti-Beclin-1 (1:1000, ab302669, Abcam, Cambridge, UK), anti-RANBP1 (1:1000, ab133550, Abcam, Cambridge, UK), anti-P13K (1:2000, ab180967, Abcam,



Table 1. Primer sequences for qRT-PCR.

Target	Direction	Sequence (5′–3′)
Notch Receptor 3 (NOTCH3)	Forward	CCTGCCTGCCTCTATGACAAC
NOTCH3	Reverse	ACACTCCTCGGTGTTACAGCC
LC3B	Forward	TGCCGTCCGAGAAAACCTTCAAAC
LC3B	Reverse	CGGGATTTTGGTAGGATGCTGCTC
p62	Forward	CTGGGAGATGGGCACACC
p62	Reverse	TGGGATCTTCCGATGGACCA
Beclin1	Forward	TCCATTACTTGCCACAGCC
Beclin1	Reverse	GCCATCAGATGCCTCCC
RAN binding protein 1 (RANBP1)	Forward	GCCGCCAAGAGGACAGTC
RANBP1	Reverse	CATGAGAAGGCGGATGGT
GAPDH	Forward	GATGACATCAAGAAGGTGGTGAAG
GAPDH	Reverse	ACCCTGTTGCTGTAGCCATATTC

qRT-PCR, quantitative real-time polymerase chain reaction; GAPDH; glyceraldehyde-3-phosphate dehydrogenase.

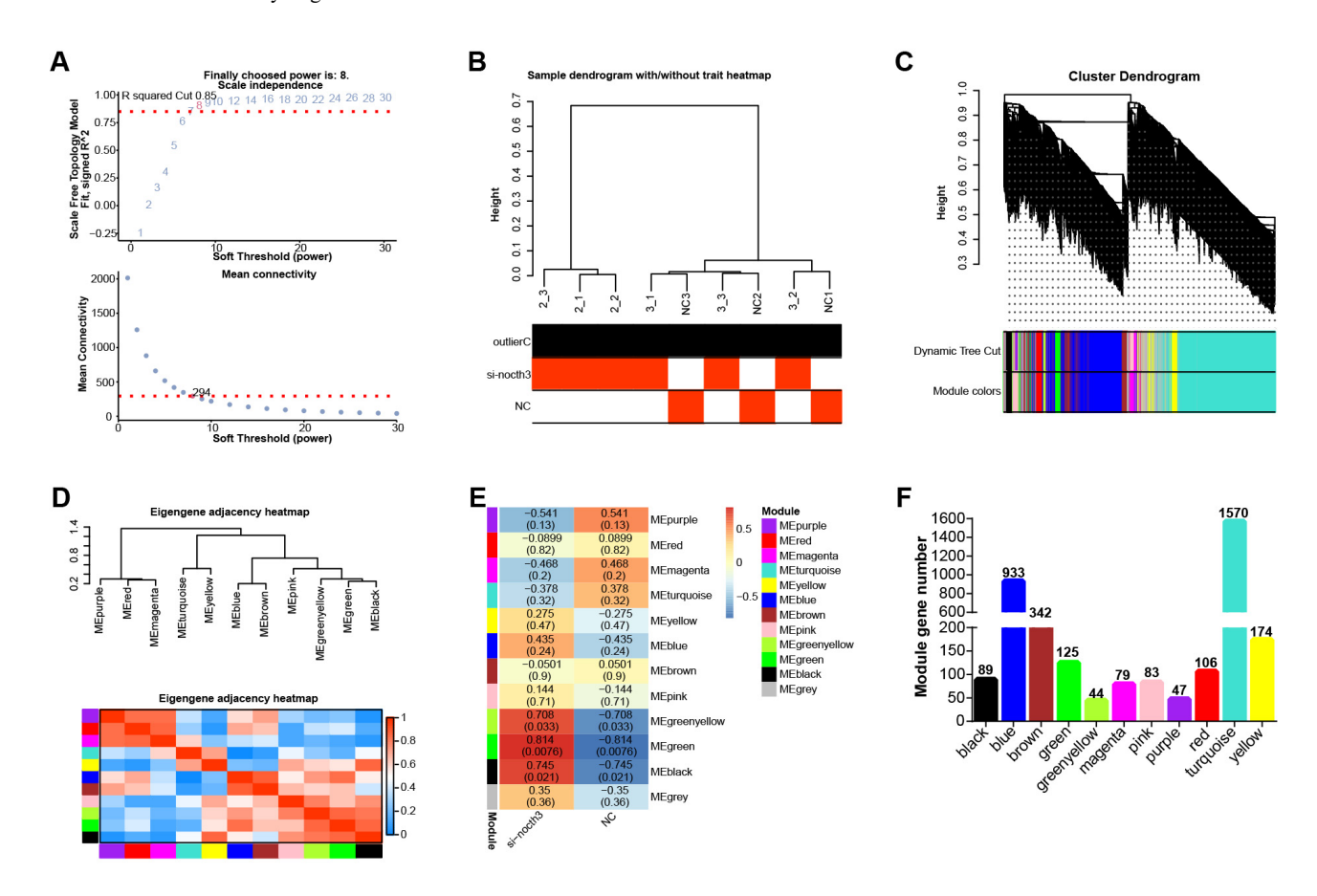


Fig. 1. WGCNA identified key modules in the VSMC sequencing data. (A) The upper figure shows the determination of the optimal soft threshold in the gene coexpression network, and the lower figure shows the mean connectivity for different soft thresholds. (B) Cluster dendrogram of nine selected samples. The dendrogram (top) illustrates the clustering of samples, and the heatmap (bottom) shows the trait distribution, where color intensity represents trait values. (C) Gene dendrogram obtained on the basis of the clustering dissimilarity of topological overlap, with different color bands corresponding to different module colors. (D) Eigengene adjacency heatmap; the redder the color is, the stronger the correlation. (E) Heatmap of the correlations between gene modules and *NOTCH3* knockdown samples. The numbers in the modules represent the correlation coefficients and *p* values. (F) Bar plot of the number of genes in each WGCNA module identified. WGCNA, weighted gene coexpression network analysis; VSMC, vascular smooth muscle cell; *NOTCH3*, Notch receptor 3.

Cambridge, UK), anti-p-PI3K (1:1000, ab138364, Abcam, Cambridge, UK), anti-AKT (1:2000, ab8805, Abcam, Cambridge, UK) and anti-p-AKT (1:1000, ab38449, Abcam, Cambridge, UK).

2.12 Statistical Analysis

The R software suite was utilized for conducting the statistical analysis. The mean \pm standard error was adopted to demonstrate all the results (p < 0.05). Pairwise comparisons were analyzed via Student's t test. The experiments were repeated at least three times.

3. Results

3.1 Key Modules of WGCNA were Determined to be Turquoise Modules

With respect to the data provided by the sequencing company, the WGCNA algorithm was used to create a gene coexpression network, with the optimal soft threshold set at $\beta = 8$ (Fig. 1A). An in-depth examination of the clustering of nine selected samples was subsequently conducted (Fig. 1B). The genes were subsequently classified into distinct modules, and a hierarchical clustering dendrogram of genes was constructed (Fig. 1C,D). Further analysis of the correlations between gene modules and sample traits through a heatmap revealed that the green module presented the highest correlation (r = 0.814) with the samples (Fig. 1E). Additionally, the adjacency heatmap of feature genes revealed interconnections between gene modules. Moreover, the results in Fig. 1F show the number of genes corresponding to each module, among which the turquoise module has the greatest number of genes. In summary, the screening process within the gene coexpression network identified the turquoise module as the pivotal module for subsequent analysis.

3.2 Expression of Overlapping Genes and Screening of Hub Genes in NOTCH3-Knockdown VSMC Samples

On the basis of the FC and *p* value screening criteria, 579 DEGs were identified from 9 samples, including 301 upregulated DEGs and 278 downregulated DEGs (Fig. 2A). Next, 38 overlapping genes were identified between the 579 DEGs and the turquoise module (Fig. 2B and **Supplementary Table 1**). These overlapping genes formed a PPI network with 11 nodes and 6 edges (Fig. 2C). Notably, genes such as *HPF1*, *CRNKL1*, *RANBP1*, *CENPS*, and *HIST1H4L* showed the maximum AUC value of 1, and the AUC values of the remaining genes were all greater than the significance threshold of 0.7, indicating that these genes have high diagnostic value (Fig. 2D). Furthermore, significant downregulation of the expression of these 11 genes was observed in the si-*NOTCH3*-treated samples (Fig. 2E). In this study, we selected the *RANBP1* gene for subsequent research.

3.3 NOTCH3 Knockdown Affects the Proliferation, Apoptosis and Cell Cycle of VSMCs

By qRT-PCR and WB, we systematically investigated the expression levels of NOTCH3 in various VSMCs, including PASMCs, HASMCs, and HUASMCs. NOTCH3 was significantly upregulated in VSMCs, particularly in HASMCs and HUASMCs (Fig. 3A-C). Consequently, HASMCs and HUASMCs were chosen for subsequent experiments. Subsequent knockdown of NOTCH3 in HASMCs and HUASMCs was confirmed by qRT-PCR and WB, which demonstrated effective downregulation (Fig. 3D-F). Proliferation assays via the CCK-8 method revealed significant inhibition of cell proliferation in HASMCs and HUASMCs after NOTCH3 knockdown (Fig. 3G,H). Flow cytometry analysis revealed a notable increase in the percentage of apoptotic HASMCs and HUASMCs following NOTCH3 knockdown (Fig. 3I-K), accompanied by cell cycle arrest in the S phase (Fig. 3L-O).

3.4 Dose-Dependent Effects of HG on NOTCH3 and p-mTOR Expression in VSMCs

Vascular remodeling and inflammation are two frequent cardiovascular processes that are linked to activation of the mTOR signaling pathway [21]. As a pivotal signaling molecule in the regulation of cellular autophagy, the suppression of mTOR activity can initiate autophagic processes, which, in VSMCs, may further influence cell viability [22]. To evaluate the effect of HG on VSMC survival, cells were treated with glucose at different concentrations (5.5, 10.5, 15.5 and 25.5 mM). WB revealed a dose-dependent increase in NOTCH3 protein levels and a dose-dependent decrease in p-mTOR expression in VSMCs treated with 10.5, 15.5 and 25.5 mM glucose compared with those treated with 5.5 mM glucose (Fig. 4A–F). These findings suggest that higher glucose concentrations can significantly upregulate NOTCH3 while downregulating pmTOR. Therefore, we selected a glucose concentration of 25.5 mM for use in further research. Further WB analysis revealed that as the duration of glucose treatment increased, NOTCH3 expression gradually increased significantly in HASMCs and HUASMCs, and p-mTOR expression decreased accordingly (Fig. 4G-L). Notably, while mTOR expression levels remained relatively stable, the decrease in p-mTOR reflects a reduction in its activated form, indicating suppression of the mTOR signaling pathway over time with high-glucose treatment.

3.5 Impact of Varying Glucose Concentrations on Autophagy in VSMCs

The viability of HASMCs and HUASMCs following 24 hours of treatment with various concentrations of glucose was assessed via the CCK-8 assay (Fig. 5A,B). Notably, cell viability significantly decreased with increasing glucose concentration. To investigate the influence of different glucose concentrations on VSMC autophagy, qRT-



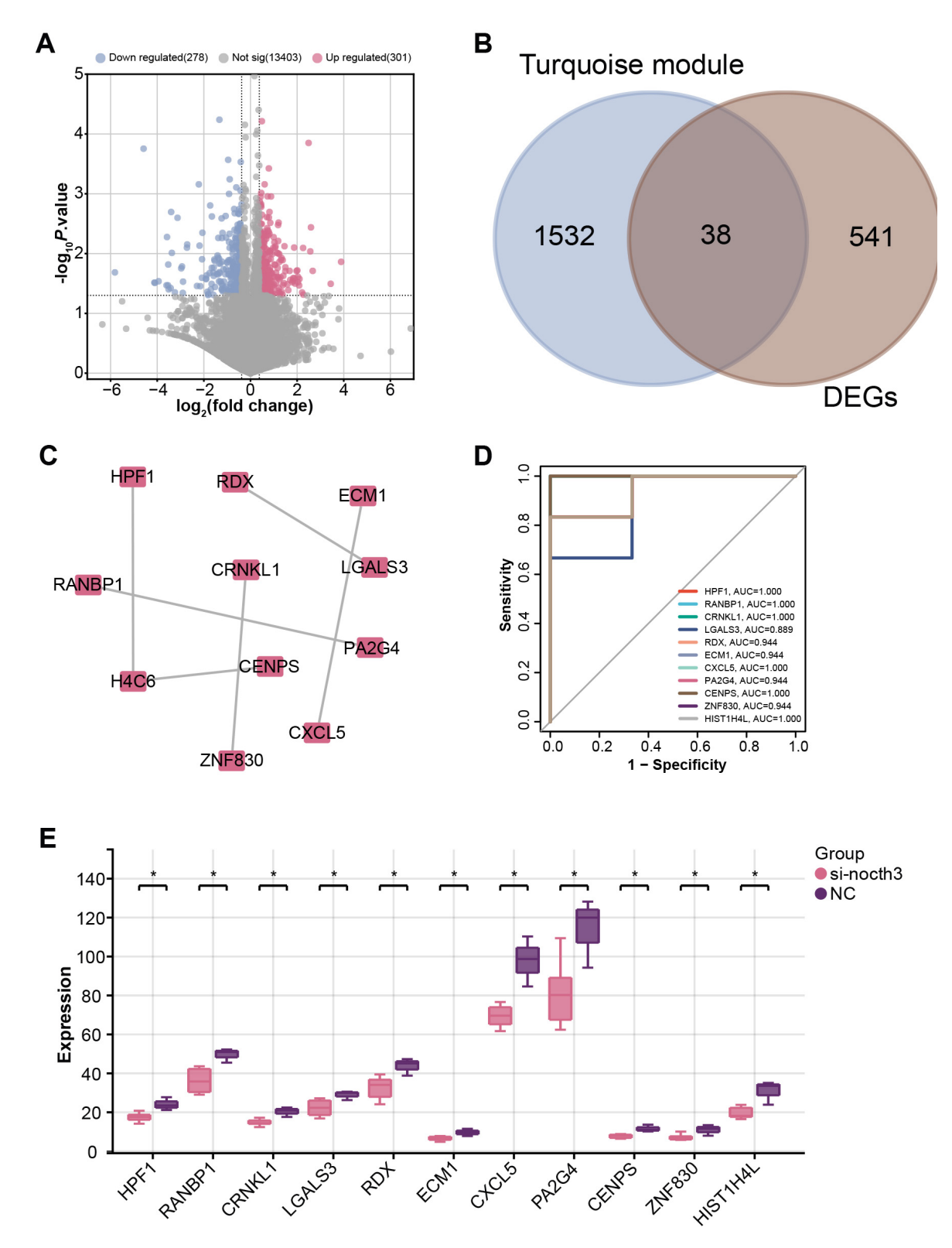


Fig. 2. Screening, clinical diagnostic value and expression analysis of 11 candidate genes. (A) Volcano plot depicting the results of differential gene expression analysis. Red represents upregulated DEGs, and purple represents downregulated DEGs. (B) Venn diagram of the intersection of the turquoise module and DEGs. (C) PPI network with 11 nodes and 6 edges. Nodes represent genes, and edges represent interconnections between genes. (D) ROC curve analysis of 11 key genes. A higher AUC indicates greater clinical diagnostic relevance of the gene. (E) Boxplot of the expression analysis of 11 genes. The red box line represents the si-*NOTCH3* group, and the purple box line represents the NC group. *p < 0.05. PPI, protein-protein interaction; DEGs, differentially expressed genes; AUC, area under the curve; ROC, Receiver Operating Characteristic; NC, negative control.

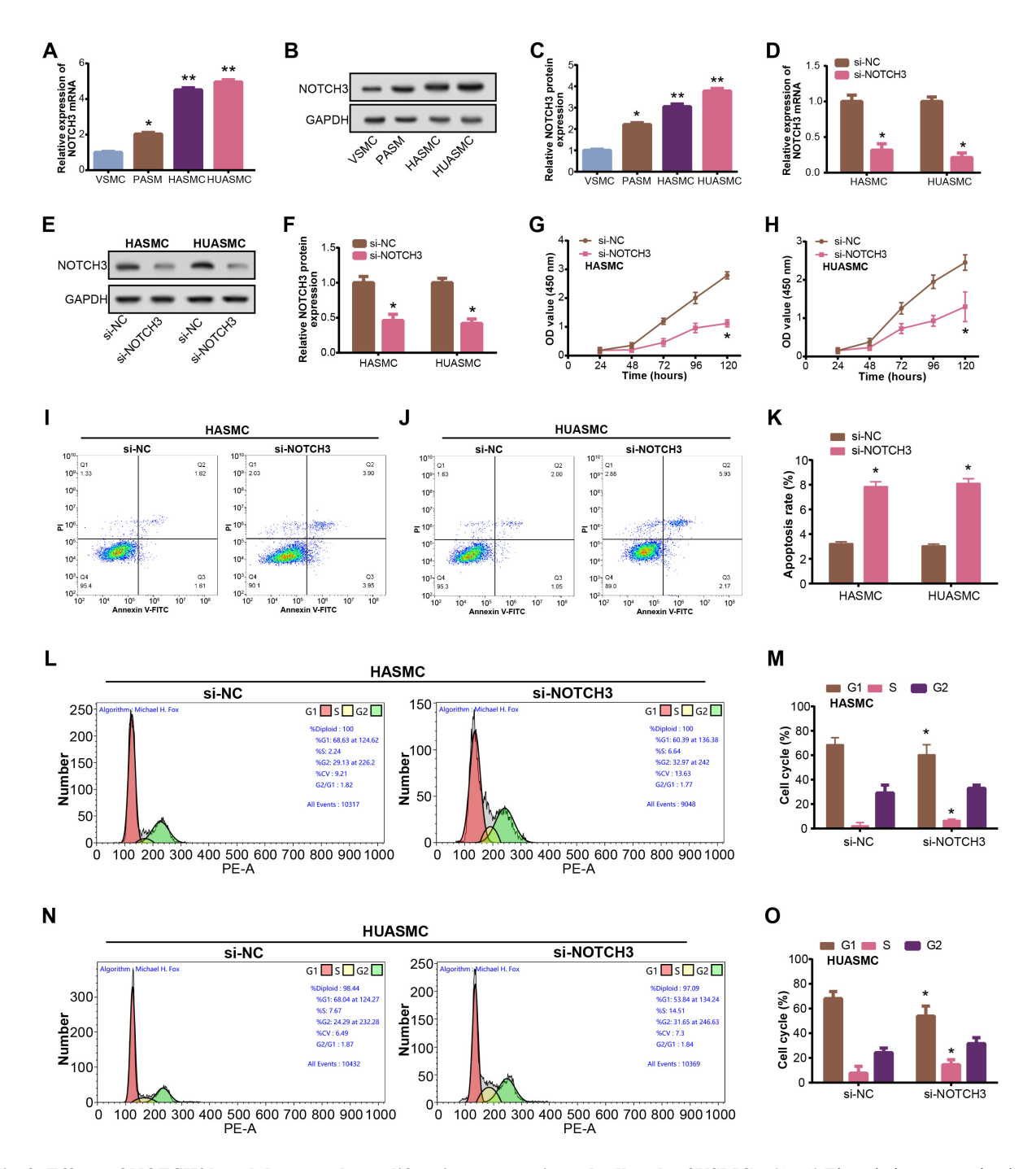


Fig. 3. Effects of *NOTCH3* knockdown on the proliferation, apoptosis, and cell cycle of VSMCs. (A–C) The relative expression level of NOTCH3 in VSMCs was detected via qRT-PCR and WB. VSMCs included PASMCs, HASMCs, and HUASMCs. (D–F) Detection of *NOTCH3* knockdown efficiency in HASMCs and HUASMCs via qRT-PCR and WB. (G,H) The CCK-8 method was used to detect the effect of si-*NOTCH3* on HASMC and HUASMC proliferation. (I–K) Flow cytometry was used to detect the percentage of apoptotic HASMCs before and after *NOTCH3* knockdown. (L–O) Flow cytometry was used to detect the cell cycle status of HASMCs before and after *NOTCH3* knockdown. *p < 0.05, **p < 0.01. qRT-PCR, quantitative real-time polymerase chain reaction; WB, western blotting.

PCR and WB were used to measure the mRNA and protein expression levels of autophagy-related factors in VSMCs (Fig. 5C–H). Compared with the 5.5 mM glucose treatment group, the 10.5, 15.5, and 25.5 mM glucose treatment groups presented significant increases in LC3B (LC3 I/LC3 II) and Beclin-1 expression at both the mRNA and protein

levels. Concurrently, the mRNA and protein expression levels of p62 significantly decreased. These results indicate that high-glucose concentrations exacerbate autophagic activity in VSMCs, as evidenced by the altered expression of key autophagy-related factors.



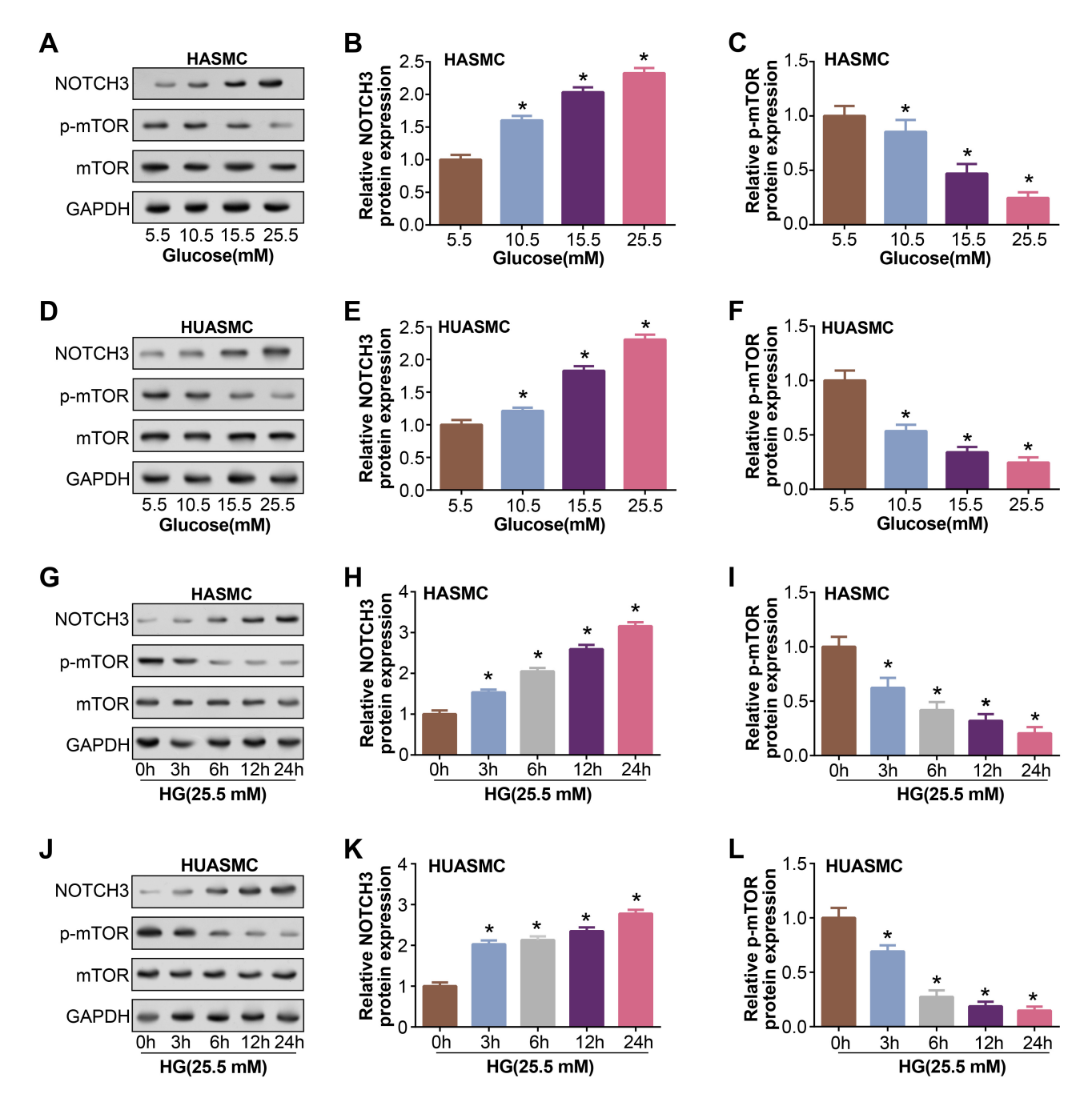


Fig. 4. Effects of the NOTCH3 and mTOR signaling pathways on VSMCs. (A–F) WB detection of NOTCH3, p-mTOR, and mTOR expression in HASMCs and HUASMCs after treatment with different concentrations (5.5 mM, 10.5 mM, 15.5 mM, and 25.5 mM) of glucose. (G–L) WB detection of NOTCH3, p-mTOR, and mTOR expression in HASMCs and HUASMCs after treatment with 25.5 mM glucose for 0, 3, 6, 12, and 24 hours. *p < 0.05.

3.6 Impact of Various Durations of HG Treatment on VSMC Autophagy

To further explore the effects of various durations of HG treatment on autophagy, VSMCs were exposed to 25.5 mM glucose for 0, 3, 6, 12, and 24 hours. The protein and mRNA expression levels of LC3, p62, and Beclin-1 in VSMCs were assessed via WB and qRT-PCR (Fig. 6A–F). Compared with those in the 0-hour treatment group, significant increases in both the mRNA and protein levels of

LC3B (LC3 I/LC3 II) and Beclin-1 were detected in the 3-, 6-, 12-, and 24-hour treatment groups. Conversely, the mRNA and protein expression levels of p62 substantially decreased over the same time intervals.

3.7 Knockdown of NOTCH3 Inhibits HG-Induced VSMC Proliferation and Autophagy

The results of qRT-PCR and WB analysis revealed that, compared with that after treatment with the siRNA



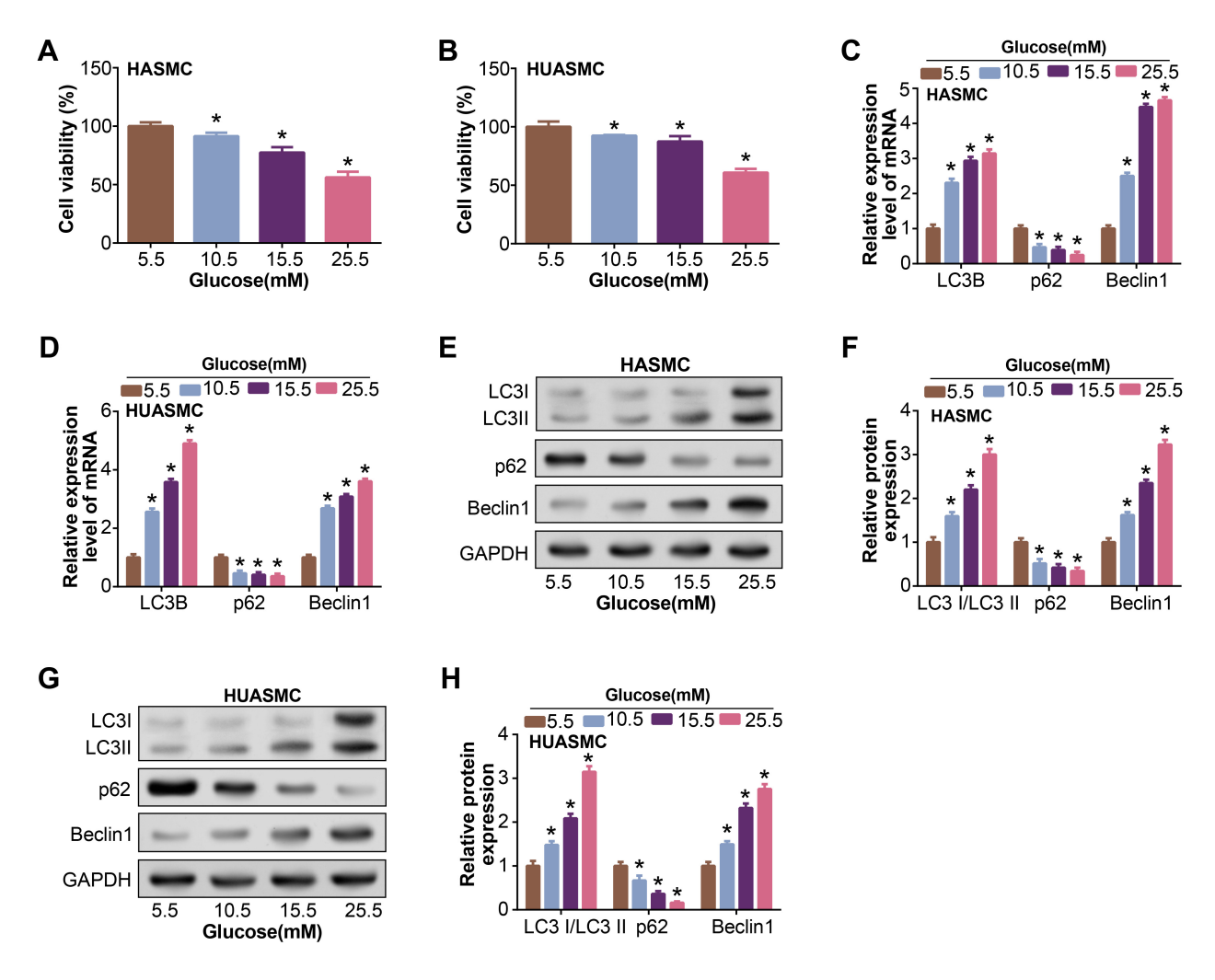


Fig. 5. Effects of different concentrations of glucose on autophagy in VSMCs. (A,B) CCK-8 detection of the viability of HASMCs and HUASMCs after treatment with different concentrations of glucose (5.5 mM, 10.5 mM, 15.5 mM, and 25.5 mM) for 24 hours. (C–H) qRT-PCR and WB were used to detect the expression levels of autophagy-related markers in HASMCs and HUASMCs after treatment with different concentrations of glucose (5.5 mM, 10.5 mM, 15.5 mM, and 25.5 mM). *p < 0.05.

negative control (si-NC), the expression of NOTCH3 was upregulated after 24 hours of treatment with 25.5 mM glucose. After the addition of si-NOTCH3, the HG-mediated upregulation of NOTCH3 expression was significantly inhibited (Fig. 7A–C). The assessment of cell viability via the CCK-8 assay revealed that HG treatment attenuated cell viability, and subsequent knockdown of NOTCH3 further led to a decrease in cell viability (Fig. 7D,E). WB analysis revealed that HG treatment caused a significant increase in autophagic LC3 I/LC3 II and Beclin-1 protein levels, and the addition of si-NOTCH3 alleviated this effect. In contrast, HG treatment resulted in a significant decrease in p62 protein levels in VSMCs, and this effect was reversed upon the addition of si-NOTCH3 (Fig. 7F–I).

3.8 Knockdown of RANBP1 Inhibits the Proliferation of VSMCs and Promotes Apoptosis

qRT-PCR and WB analyses revealed a significant decrease in RANBP1 expression in VSMCs after NOTCH3

was knocked down (Fig. 8A–C). The efficiency of *RANBP1* knockdown was further validated through qRT-PCR and WB assays, with si-*RANBP1* #1 demonstrating superior knockdown efficiency; thus, it was selected for subsequent experiments (Fig. 8D–F). *RANBP1* knockdown inhibited cell proliferation, as detected by CCK-8 assay (Fig. 8G,H). Moreover, flow cytometry revealed that the apoptosis rate was significantly increased after *RANBP1* knockdown, further indicating that *RANBP1* is involved in the regulation of VSMC survival (Fig. 8I–K).

3.9 Effects of the RANBP1/NOTCH3 Axis on HG-Stimulated VSMCs

Validation through qRT-PCR and WB confirmed the effective overexpression of *RANBP1* in VSMCs (Fig. 9A–C). Subsequent qRT-PCR and WB analyses revealed significant upregulation of *RANBP1* expression in VSMCs upon exposure to HG. The addition of si-*NOTCH3* attenuated this increase, whereas the introduction of *RANBP1* overexpres-



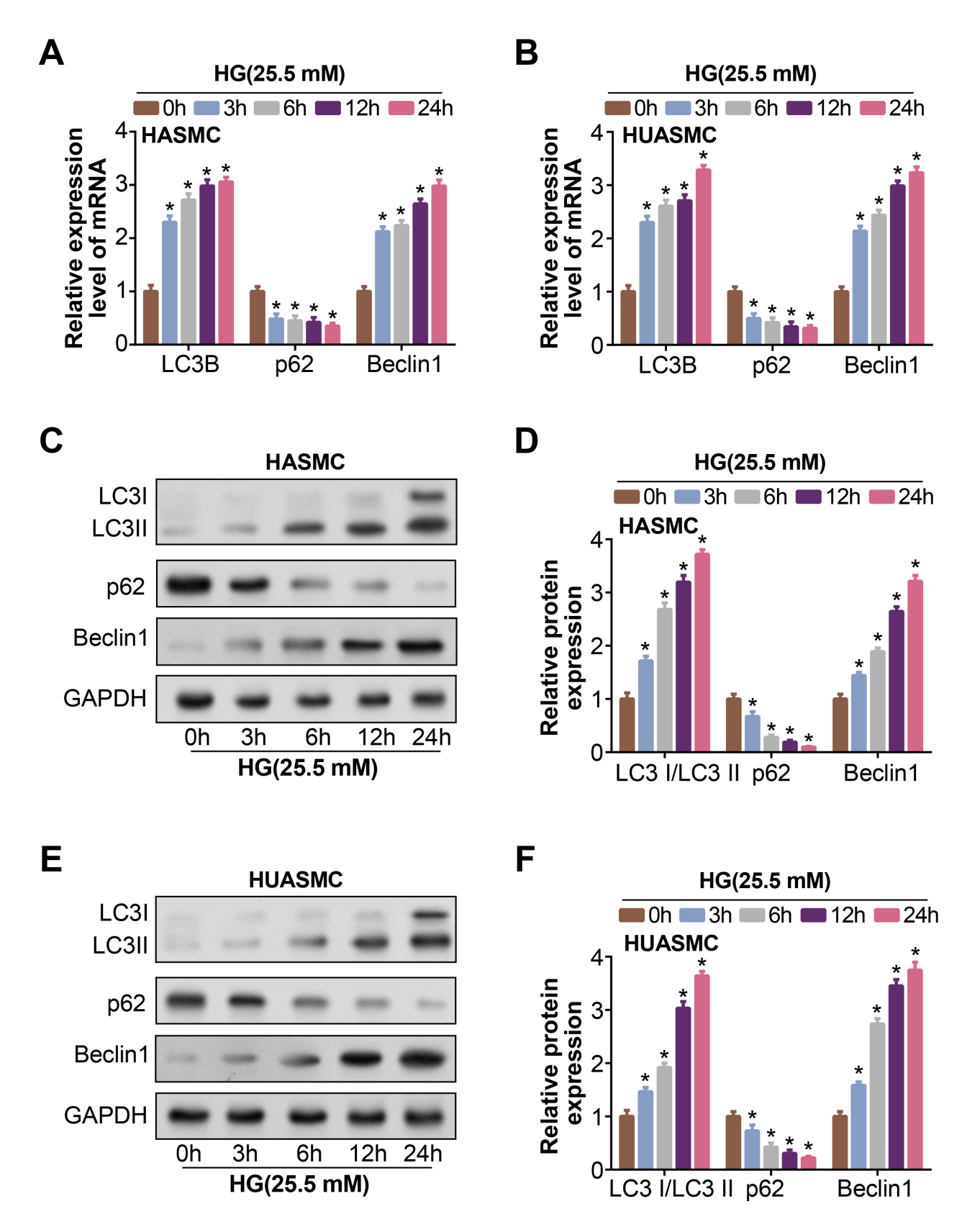


Fig. 6. Effects of different durations of HG treatment on autophagy in VSMCs. (A,B) qRT–PCR was used to detect the expression levels of the autophagy-related proteins LC3B, p62, and Beclin-1 in HASMCs and HUASMCs after treatment with 25.5 mM glucose for 0, 3, 6, 12, and 24 hours. (C–F) WB detection of the expression levels of the autophagy-related proteins LC3 I/LC3 II, p62, and Beclin-1 in HASMCs and HUASMCs after treatment with 25.5 mM glucose for 0, 3, 6, 12, and 24 hours. * *p < 0.05.

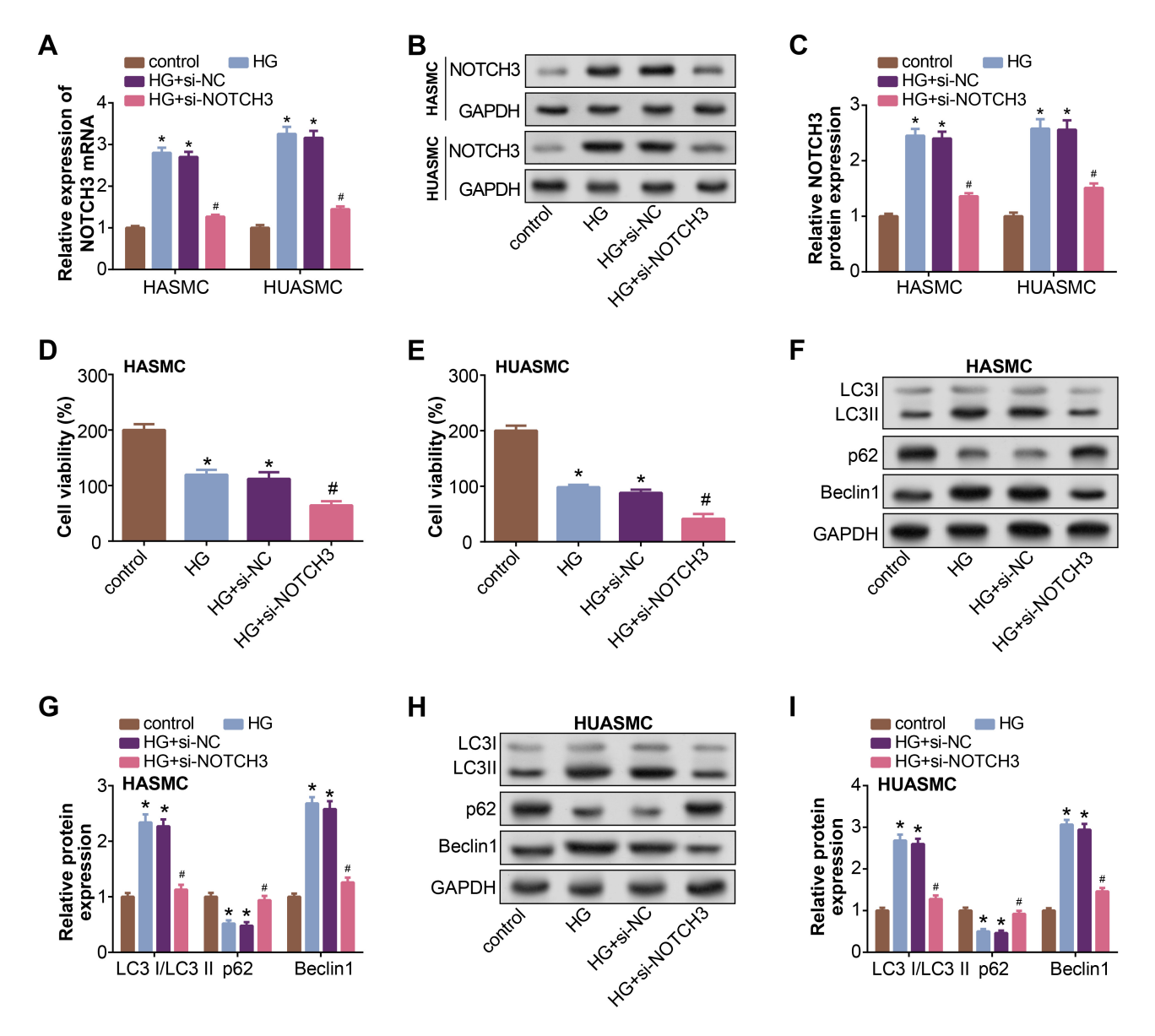


Fig. 7. Effects of *NOTCH3* knockdown on HG-induced proliferation and autophagy in VSMCs. (A–C) VSMCs were treated with 25.5 mM glucose for 24 hours. After *NOTCH3* was knocked down, qRT-PCR and WB were used to detect the knockdown efficiency of NOTCH3. (D,E) The CCK-8 method was used to detect the viability of HASMCs and HUASMCs treated with 25.5 mM glucose for 24 hours and *NOTCH3* knockdown. (F–I) WB was used to detect the expression of autophagy-related proteins in HASMCs and HUASMCs after *NOTCH3* knockdown and 25.5 mM glucose treatment for 24 hours. *p < 0.05. #p < 0.05.

sion plasmids amplified this increase (Fig. 9D–H). The results of the cell viability test revealed that HG significantly reduced cell viability. Under HG conditions, downregulation of *NOTCH3* led to a further reduction in cell viability. On this basis, the overexpression of *RANBP1* could partially counteract both of their detrimental effects on cell viability (Fig. 9I,J). Similarly, the WB results (Fig. 9K–N) revealed that *RANBP1* overexpression counteracted the significant decrease in LC3 and Beclin-1 expression induced by si-*NOTCH3*. Furthermore, it reversed the large increase in p62 and p-mTOR expression caused by si-*NOTCH3*. After HG induction, the levels of the autophagy-related markers LC3 I/LC3 II and Beclin-1 increased, whereas

the levels of p62 and p-mTOR decreased, indicating increased autophagic flux. After knocking down *NOTCH3* in the presence of HG, we observed a significant decrease in the levels of LC3 II/I and Beclin-1 and the restoration of p62 and p-mTOR protein levels, suggesting that *NOTCH3* may play a role in HG-induced autophagy. In HG-treated cells with *NOTCH3* knockdown, the overexpression of *RANBP1* reversed the HG-induced changes in the expression of autophagy-related markers, with increased levels of LC3 I/LC3 II and Beclin-1 but decreased p62 and p-mTOR protein levels. Our results indicate that *RANBP1* is a key regulator of the *NOTCH3*-mediated autophagy pathway in VSMCs under HG conditions. The overexpression



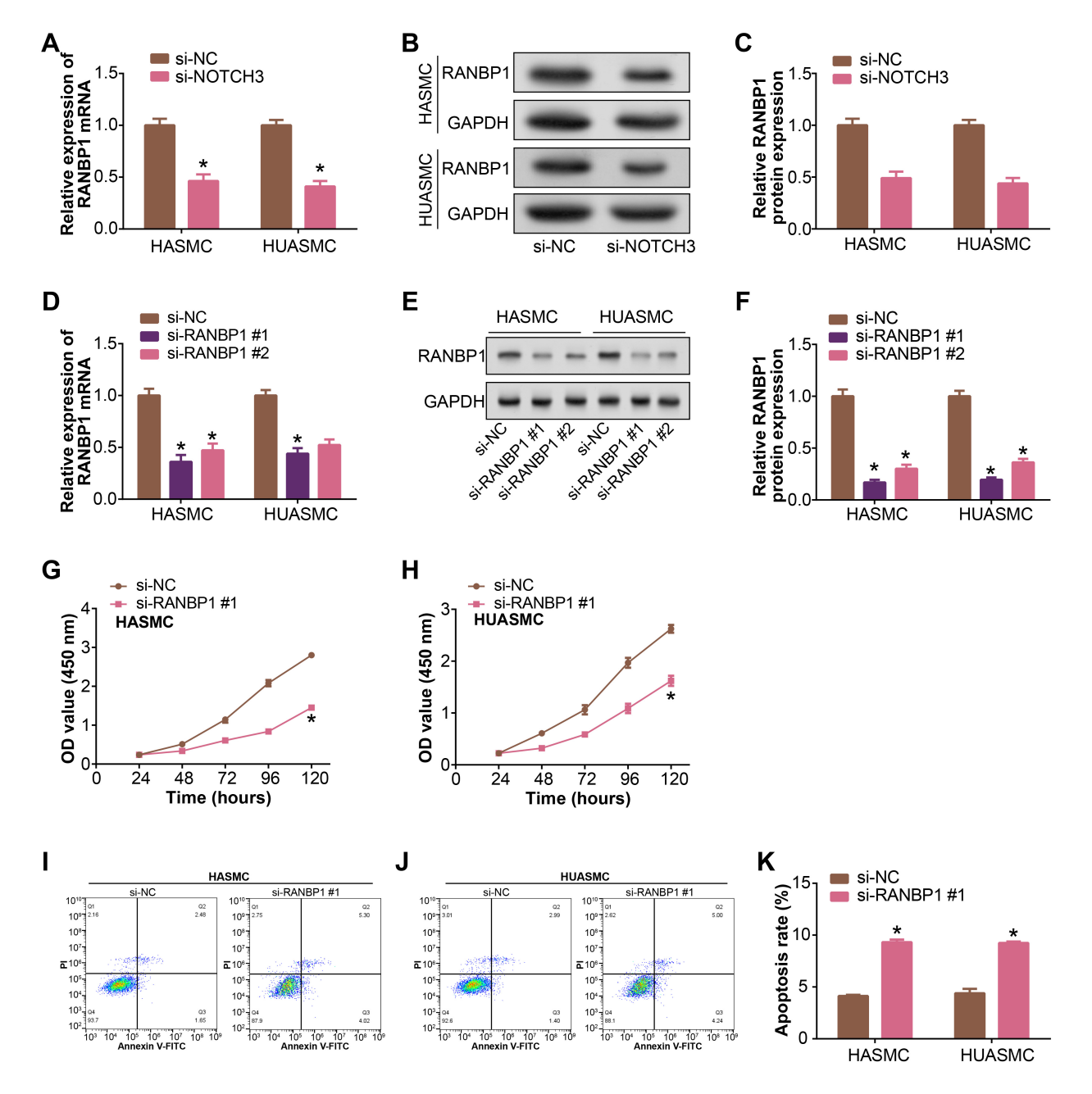


Fig. 8. Effects of *RANBP1* knockdown on VSMC proliferation and apoptosis. (A–C) The mRNA and protein expression levels of RANBP1 in HASMCs and HUASMCs after NOTCH3 knockdown were detected via qRT-PCR and WB. (D–F) Detection of *RANBP1* knockdown efficiency (si-*RANBP1* #1, si-*RANBP1*#2) in HASMCs and HUASMCs by qRT-PCR and WB. (G,H) CCK-8 assay was used to detect the effect of *RANBP1* knockdown on HASMC and HUASMC proliferation. (I–K) Flow cytometry was used to detect apoptosis in HASMCs and HUASMCs after *RANBP1* knockdown. *p < 0.05.

of *RANBP1* can alleviate HG-induced changes in autophagy and viability, suggesting its potential as a protective mechanism against glucose-induced toxicity in vascular pathophysiology.

The PI3K/Akt/mTOR pathway is known to play a crucial role in regulating autophagy [23]. We assessed the expression of key proteins in this pathway following HG treatment, *NOTCH3* knockdown, and *RANBP1* overexpression. The results showed that under HG conditions, the phospho-

rylation levels of PI3K, Akt, and mTOR were decreased, suggesting an increase in autophagic flux. Interestingly, when *NOTCH3* was knocked down in the presence of HG, the phosphorylation levels of PI3K, Akt, and mTOR were restored. Moreover, the overexpression of *RANBP1* reversed the effects of *NOTCH3* knockdown. These findings suggest that *NOTCH3* and *RANBP1* may play roles in regulating HG-induced autophagy through the PI3K/Akt/mTOR pathway (**Supplementary Fig.1**).



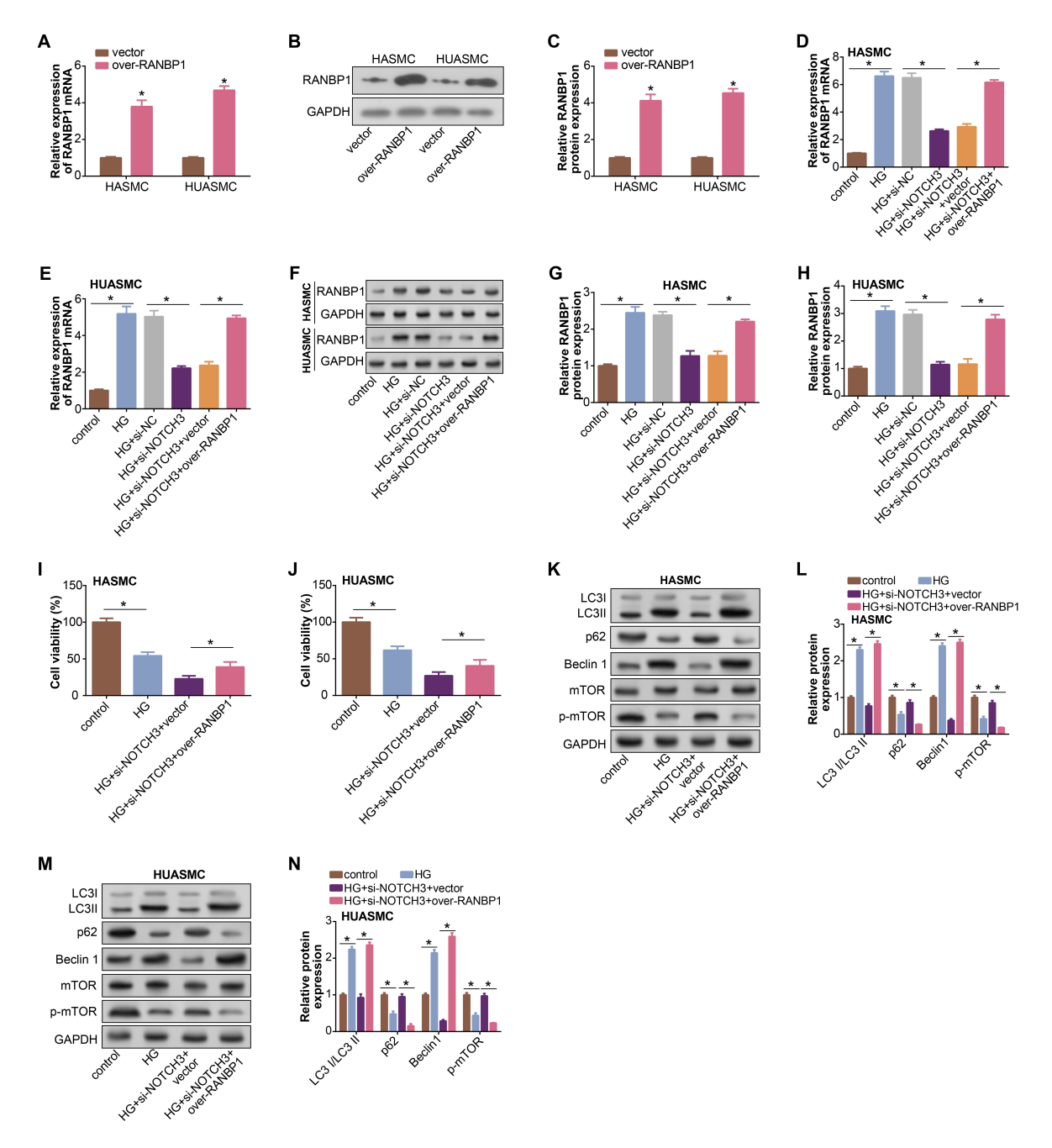


Fig. 9. Effects of the RANBPI/NOTCH3 axis on HG-stimulated VSMCs. (A–C) The overexpression efficiency of RANBP1 in HASMCs and HUASMCs was measured by qRT-PCR and WB. (D–H) qRT-PCR and WB were used to detect the expression level of RANBP1 in HASMCs and HUASMCs. The groups were as follows: control; HG; HG+si-NC; HG+si-NOTCH3; HG+ si-NOTCH3+vector; and HG+ si-NOTCH3+over-RANBP1. (I,J) CCK-8 detection of HASMCs and HUASMCs after different treatments. The groups were as follows: control; HG; HG+si-NOTCH3+vector; and HG+si-NOTCH3+over-RANBP1. (K–N) WB was used to detect the expression of autophagy-related markers (LC3 I/LC3 II, p62, Beclin-1, mTOR, and p-mTOR) in HASMCs and HUASMCs. The groups were as follows: control; HG; HG+si-NOTCH3+vector; and HG+si-NOTCH3+over-RANBP1. *p < 0.05. The glucose concentration under HG conditions was 25.5 mM.

4. Discussion

Vascular smooth muscle cells (VSMCs), which are found mainly in the walls of human arteries and veins, are the primary cell constituents and are responsible for maintaining vascular tension [24]. Many cardiovascular disor-

ders, including hypertension, atherosclerosis, and restenosis following angioplasty, are cytopathologically based on the structural and functional alterations of VSMCs [25]. Therefore, research on VSMCs is important for treating smooth muscle-related diseases.



Percutaneous coronary intervention is important for the treatment of patients with coronary heart disease, and drug-eluting stents (DESs) can inhibit the growth of VSMCs and effectively reduce the stenosis rate in the stent by inhibiting endovascular hyperproliferation [26]. However, advanced in-stent restenosis is still observed clinically, so it is necessary to find more effective biological targets. Previous studies have shown that NOTCH3 is associated with various cancers [27,28] in terms of tumor invasiveness, maintainability and chemotherapeutic resistance. Overexpression of NOTCH3 leads to zinc finger E-box-binding homeobox 1 (ZEB-1) activity, reduces Ecadherin expression, and increases fibronectin expression, thereby contributing to the epithelial-mesenchymal transition (EMT) and tumor invasion [29]. Research by Kennard S et al. [18] has shown that TGF- β 1 promotes the expression of smooth muscle cell differentiation genes through the inhibition of Notch3 and the activation of Hes1. The mechanism of action of NOTCH3 in VSMCs and cancer cells is similar, but there are also differences. In this study, we investigated the molecular mechanism of NOTCH3 in VSMCs.

On the basis of the sequencing analysis, we performed WGCNA on all genes in the sequencing samples provided by the sequencing company and selected the turquoise module for analysis. Moreover, we screened DEGs from these samples, identified those that intersected, performed bioinformatics analysis on the overlapping genes, and identified the hub gene *RANBP1*.

HG refers to elevated glucose levels in the cellular environment, which is known to impact cellular signaling pathways [30]. The NOTCH-mTOR signaling pathway involves interactions between NOTCH receptors and the mammalian target of rapamycin (mTOR), regulating various cellular processes [31]. A study [32] suggests that HG can activate the NOTCH-mTOR signaling pathway. NOTCH receptors, particularly NOTCH3, respond to highglucose stimulation and contribute to cellular responses, such as autophagy and calcification. The mTOR signaling pathway, a key regulator of cellular growth and metabolism, has been implicated as a mediator in these processes [33]. Lin X et al. [34] revealed that exosomal NOTCH3 originating from high glucose-stimulated endothelial cells is pivotal in promoting VSMC calcification and aging. This process involves activation of the mTOR signaling pathway as a key mediator. We conducted in vitro cell experiments and found that knocking down NOTCH3 reduced the viability and increased the apoptosis of VSMCs. Additionally, the NOTCH3 and mTOR signaling pathways in VSMCs were activated by HG. These findings are similar to those of Cui Y et al. [35], who reported that the combination of HG and lipopolysaccharide (LPS) can trigger autophagy through the NOTCH3/mTOR signaling pathway in bovine kidney epithelial cells. In a related context, the same researchers reported that high glucose alone induces autophagy in bovine

kidney epithelial cells via the NOTCH3-mediated mTOR signaling pathway, as evidenced by changes in cell viability, LC3 and Beclin-1 expression, and p-mTOR levels [36]. The interplay between high glucose and the NOTCHmTOR signaling pathway has been investigated in different cell types, providing insights into the molecular mechanisms underlying cellular responses to elevated glucose levels. Understanding these pathways is crucial to unraveling the complexities of cellular behavior under hyperglycemic conditions, with potential implications for various physiological and pathological processes. In summary, our in vitro studies confirmed that HG conditions promote activation of the NOTCH3/mTOR signaling pathway, which plays a significant role in mediating VSMC responses, highlighting the potential of this pathway to target HG-induced vascular complications.

Autophagy-related proteins, including LC3I, LC3II, p62, and Beclin-1, play key roles in autophagy, a cellular mechanism for degrading and recycling cellular components [37]. LC3I is a cytoplasmic form of LC3, and during autophagy, it undergoes lipidation to become LC3II [38]. The conversion of LC3I to LC3II is a crucial step in autophagosome formation. LC3II is the lipidated form of LC3, which is recruited to the autophagosomal membrane. The level of LC3II is commonly used as a marker of autophagic activity. p62 is a selective substrate of autophagy and serves as a link between ubiquitinated cargo and autophagosomes [39]. It interacts with LC3, facilitating the engulfment of ubiquitinated proteins into autophagosomes for degradation [40]. One of the main players in the class III phosphatidylinositol 3-kinase complex that initiates autophagy is Beclin-1 [41]. It participates in the nucleation of the autophagosome and is crucial for the early stages of autophagy induction [42]. These proteins collectively regulate the dynamic process of autophagy, ensuring the proper elimination of damaged organelles and proteins, thereby maintaining cellular homeostasis and contributing to overall cell health. Metformin, as studied by Qiu X et al. [43], alleviates β -glycerophosphate-induced VSMC calcification through AMPK/mTOR-mediated autophagy, as demonstrated by reduced calcium deposition and altered expression of autophagy-related proteins and markers of calcification. Additionally, Tan P et al. [44] reported that the rapamycin-induced downregulation of miR-30a inhibits VSMC senescence by upregulating Beclin-1 and promoting autophagy, suggesting a potential therapeutic strategy for senescence-related cardiovascular diseases. Furthermore, Qu Y et al. [45] revealed that resveratrol hinders abdominal aortic aneurysm progression by upregulating HMOX1 and inhibiting matrix degradation, apoptosis, autophagy, and inflammation in VSMCs induced by angiotensin II, providing insights into a potential therapeutic mechanism. Our study revealed that treating VSMCs with 25.5 mM glucose for 24 h had the most obvious effect on autophagy-related proteins. Furthermore, the knockdown



of *NOTCH3* inhibited the HG-induced proliferation and autophagy of VSMCs, highlighting the subtle interplay of elevated glucose concentrations and *NOTCH3* expression in the regulation of vascular cell homeostasis.

RANBP1 is a human gene that encodes a protein involved in nucleocytoplasmic transport and the regulation of the Ran-GTPase cycle [46]. It is essential for various cellular processes, including the transport of proteins across the nuclear envelope and the modulation of cell cycle progression [15]. In a study by Zhang MS et al. [47], RANBP1 was identified as a key player in mitotic spindle assembly, controlling the amount and location of mitotic Ran-GTP production, which guarantees the accurate completion of Ran-dependent mitotic processes. The Rev-mediated posttranscriptional regulation of human immunodeficiency virus type 1 is hampered by mutations in the nuclear export signal of the human ran-binding protein RANBP1, according to research by Zolotukhin AS et al. [48]. This finding suggests a competitive interaction between Rev and RANBP1 in the nuclear export pathway. Moreover, the research conducted by Yau KC et al. [15] further supports the significant role of RANBP1 in mitotic regulation, specifically in controlling the spatial dynamics of RCC1 in human somatic cells during mitosis and ensuring the accurate execution of Ran-dependent mitotic events. Our study revealed that the RANBP1/NOTCH3 axis can serve as a key regulator of autophagy and cell survival in VSMCs under HG-induced stress. Among them, RANBP1 overexpression alleviated the harmful effects of hyperglycemia, indicating its therapeutic potential in combating HG-induced vascular injury.

The PI3K/Akt/mTOR pathway is a critical regulator of cellular metabolism and autophagy, and its dysregulation has been implicated in various pathological conditions, including diabetes-related vascular complications [49]. Our findings suggest that the RANBP1/NOTCH3 axis may intersect with this pathway to modulate autophagy under HG conditions. Specifically, we observed changes in the phosphorylation levels of PI3K, Akt, and mTOR in response to HG treatment and NOTCH3 knockdown, indicating possible crosstalk between these signaling molecules. The precise mechanisms require further investigation, but our data support a model in which *RANBP1* and *NOTCH3* influence autophagic flux through the PI3K/Akt/mTOR pathway, thereby impacting VSMC survival and function under HG conditions.

While our study provides valuable insights into the role of the *RANBP1/NOTCH3* axis in regulating autophagy under high-glucose conditions in vascular smooth muscle cells (VSMCs), there are limitations that should be acknowledged. First, our work focused primarily on *in vitro* experiments, which may not fully replicate the complexity of *in vivo* environments. Second, the mechanisms by which *RANBP1* and *NOTCH3* interact have not been fully elucidated, particularly in the context of other signaling

pathways that may be involved. Additionally, the study is limited to a specific cell type, and the generalizability of these findings to other cell types or disease models requires further investigation. To address the limitations of our study and further advance the understanding of the RANBP1/NOTCH3 axis in the regulation of autophagy under high-glucose conditions, future research should include in vivo validation of our in vitro findings, exploration of the detailed molecular interactions between RANBP1 and NOTCH3, and expansion of the research to different cell types to determine whether the observed effects are specific to VSMCs or more broadly applicable to other cell types affected by hyperglycemic conditions. These research directions will contribute to a comprehensive understanding of the role of the RANBP1/NOTCH3 axis in autophagy induced by high glucose and offer new perspectives for the treatment of cardiovascular diseases.

5. Conclusion

In summary, our study elucidates the critical role of the RANBP1/NOTCH3 axis in the regulation of autophagy and cell viability in VSMCs under HG conditions. WGCNA identified the turquoise module as a key gene module associated with VSMC traits. In addition, a set of genes with high diagnostic value was identified, among which RANBP1 was selected as a key gene in the response of VSMCs to NOTCH3 knockdown. In vitro experimental results revealed that HG exposure can regulate the expression of autophagy-related markers and reduce the viability of VSMCs, whereas NOTCH3 knockdown can exacerbate this effect. Notably, RANBP1 overexpression attenuated HG-induced autophagy and increased cell viability, suggesting the existence of a compensatory protective response. These findings highlight the therapeutic potential of targeting the RANBP1/NOTCH3 axis to mitigate the adverse effects of hyperglycemia on VSMCs, providing new insights into diabetic vascular complications. The potential clinical application of these findings lies in the development of targeted therapies that could modulate this axis to protect against vascular damage in those with diabetes. Future research should focus on in vivo validation of these mechanisms and explore the broader implications of the RANBP1/NOTCH3 axis in other cell types and disease contexts, paving the way for novel treatment strategies in diabetes-associated vascular diseases.

Availability of Data and Materials

All the data in this study are available from the corresponding author upon reasonable request. The raw RANseq data can be found in the NCBI repository (accession number: GSE229241).

Author Contributions

ZJX and JX designed the experiments and wrote the manuscript. WJL, XW, QLZ, and LCL performed the re-



search. CL and WMH supervised the experiments and provided critical feedback on the experimental design and data interpretation. YJX and JYS analyzed the data. TMW made the figures and searched references. CLZ obtained funding acquisition, carried out project administration, designed the experiments, and revised the manuscript. All authors have reviewed and edited the manuscript and contributed to editorial changes. All authors have read and approved the final manuscript. All authors have participated sufficiently in the work and agreed to be accountable for all aspects of the work.

Ethics Approval and Consent to Participate

Not applicable.

Acknowledgment

Not applicable.

Funding

This study was supported by grants from the Lishui Science and Technology Bureau (2020SJZC060).

Conflict of Interest

The authors declare no conflict of interest.

Supplementary Material

Supplementary material associated with this article can be found, in the online version, at https://doi.org/10.31083/FBL26850.

References

- [1] Frismantiene A, Philippova M, Erne P, Resink TJ. Smooth muscle cell-driven vascular diseases and molecular mechanisms of VSMC plasticity. Cellular Signalling. 2018; 52: 48–64. https://doi.org/10.1016/j.cellsig.2018.08.019.
- [2] Méndez-Barbero N, Gutiérrez-Muñoz C, Blanco-Colio LM. Cellular Crosstalk between Endothelial and Smooth Muscle Cells in Vascular Wall Remodeling. International Journal of Molecular Sciences. 2021; 22: 7284. https://doi.org/10.3390/ij ms22147284.
- [3] Elmarasi M, Elmakaty I, Elsayed B, Elsayed A, Zein JA, Boudaka A, *et al.* Phenotypic switching of vascular smooth muscle cells in atherosclerosis, hypertension, and aortic dissection. Journal of Cellular Physiology. 2024; 239: e31200. https://doi.org/10.1002/jcp.31200.
- [4] Chen R, McVey DG, Shen D, Huang X, Ye S. Phenotypic Switching of Vascular Smooth Muscle Cells in Atherosclerosis. Journal of the American Heart Association. 2023; 12: e031121. https://doi.org/10.1161/JAHA.123.031121.
- [5] Artavanis-Tsakonas S, Rand MD, Lake RJ. Notch signaling: cell fate control and signal integration in development. Science (New York, N.Y.). 1999; 284: 770–776. https://doi.org/10.1126/scienc e.284.5415.770.
- [6] Campos AH, Wang W, Pollman MJ, Gibbons GH. Determinants of Notch-3 receptor expression and signaling in vascular smooth muscle cells: implications in cell-cycle regulation. Circulation Research. 2002; 91: 999–1006. https://doi.org/10.1161/01.res. 0000044944.99984.25.

- [7] Joutel A, Andreux F, Gaulis S, Domenga V, Cecillon M, Battail N, et al. The ectodomain of the Notch3 receptor accumulates within the cerebrovasculature of CADASIL patients. The Journal of Clinical Investigation. 2000; 105: 597–605. https://doi.org/10.1172/JCI8047.
- [8] Morrow D, Guha S, Sweeney C, Birney Y, Walshe T, O'Brien C, et al. Notch and vascular smooth muscle cell phenotype. Circulation Research. 2008; 103: 1370–1382. https://doi.org/10.1161/ CIRCRESAHA.108.187534.
- [9] Sweeney C, Morrow D, Birney YA, Coyle S, Hennessy C, Scheller A, et al. Notch 1 and 3 receptor signaling modulates vascular smooth muscle cell growth, apoptosis, and migration via a CBF-1/RBP-Jk dependent pathway. FASEB Journal: Official Publication of the Federation of American Societies for Experimental Biology. 2004; 18: 1421–1423. https://doi.org/10.1096/fj.04-1700fje.
- [10] Morrow D, Scheller A, Birney YA, Sweeney C, Guha S, Cummins PM, et al. Notch-mediated CBF-1/RBP-Jkappa-dependent regulation of human vascular smooth muscle cell phenotype in vitro. American Journal of Physiology. Cell Physiology. 2005; 289: C1188–96. https://doi.org/10.1152/ajpcell.00198.2005.
- [11] Wang W, Prince CZ, Hu X, Pollman MJ. HRT1 modulates vascular smooth muscle cell proliferation and apoptosis. Biochemical and Biophysical Research Communications. 2003; 308: 596–601. https://doi.org/10.1016/s0006-291x(03)01453-0.
- [12] Zhou W, Yuan X, Li J, Wang W, Ye S. Retinol binding protein 4 promotes the phenotypic transformation of vascular smooth muscle cells under high glucose condition via modulating RhoA/ROCK1 pathway. Translational Research: the Journal of Laboratory and Clinical Medicine. 2023; 259: 13–27. https://doi.org/10.1016/j.trsl.2023.03.004.
- [13] Zhou DM, Ran F, Ni HZ, Sun LL, Xiao L, Li XQ, et al. Metformin inhibits high glucose-induced smooth muscle cell proliferation and migration. Aging. 2020; 12: 5352–5361. https://doi.org/10.18632/aging.102955.
- [14] Chen Y, Zhang H, Liu H, Li K, Jia M, Su X. High Glucose Upregulated Vascular Smooth Muscle Endothelin Subtype B Receptors via Inhibition of Autophagy in Rat Superior Mesenteric Arteries. Annals of Vascular Surgery. 2018; 52: 207–215. https://doi.org/10.1016/j.avsg.2018.02.028.
- [15] Yau KC, Arnaoutov A, Aksenova V, Kaufhold R, Chen S, Dasso M. RanBP1 controls the Ran pathway in mammalian cells through regulation of mitotic RCC1 dynamics. Cell Cycle (Georgetown, Tex.). 2020; 19: 1899–1916. https://doi.org/ 10.1080/15384101.2020.1782036.
- [16] Nicolás FJ, Moore WJ, Zhang C, Clarke PR. XMog1, a nuclear ran-binding protein in Xenopus, is a functional homologue of Schizosaccharomyces pombe mog1p that co-operates with RanBP1 to control generation of Ran-GTP. Journal of Cell Science. 2001; 114: 3013–3023. https://doi.org/10.1242/jcs.114. 16.3013.
- [17] Morris HE, Neves KB, Montezano AC, MacLean MR, Touyz RM. Notch3 signalling and vascular remodelling in pulmonary arterial hypertension. Clinical Science (London, England: 1979). 2019; 133: 2481–2498. https://doi.org/10.1042/CS 20190835.
- [18] Kennard S, Liu H, Lilly B. Transforming growth factor-beta (TGF- 1) down-regulates Notch3 in fibroblasts to promote smooth muscle gene expression. The Journal of Biological Chemistry. 2008; 283: 1324–1333. https://doi.org/10.1074/jbc. M706651200.
- [19] Pu RT, Dasso M. The balance of RanBP1 and RCC1 is critical for nuclear assembly and nuclear transport. Molecular Biology of the Cell. 1997; 8: 1955–1970. https://doi.org/10.1091/mbc.8. 10.1955.
- [20] Xu J, Sun H, Huang G, Liu G, Li Z, Yang H, et al. A fixation method for the optimisation of western blotting.



- Scientific Reports. 2019; 9: 6649. https://doi.org/10.1038/s41598-019-43039-3.
- [21] Sanches-Silva A, Testai L, Nabavi SF, Battino M, Pandima Devi K, Tejada S, et al. Therapeutic potential of polyphenols in cardiovascular diseases: Regulation of mTOR signaling pathway. Pharmacological Research. 2020; 152: 104626. https://doi.org/10.1016/j.phrs.2019.104626.
- [22] Grootaert MOJ, Moulis M, Roth L, Martinet W, Vindis C, Bennett MR, et al. Vascular smooth muscle cell death, autophagy and senescence in atherosclerosis. Cardiovascular Research. 2018; 114: 622–634. https://doi.org/10.1093/cvr/cvy007.
- [23] Wang R, Wang M, Fan YC, Wang WJ, Zhang DH, Andy Li P, et al. Hyperglycemia exacerbates cerebral ischemia/reperfusion injury by up-regulating autophagy through p53-Sesn2-AMPK pathway. Neuroscience Letters. 2024; 821: 137629. https://doi.org/10.1016/j.neulet.2024.137629.
- [24] Lacolley P, Regnault V, Segers P, Laurent S. Vascular Smooth Muscle Cells and Arterial Stiffening: Relevance in Development, Aging, and Disease. Physiological Reviews. 2017; 97: 1555–1617. https://doi.org/10.1152/physrev.00003.2017.
- [25] Wang Y, Xie Y, Zhang A, Wang M, Fang Z, Zhang J. Exosomes: An emerging factor in atherosclerosis. Biomedicine & Pharmacotherapy = Biomedecine & Pharmacotherapie. 2019; 115: 108951. https://doi.org/10.1016/j.biopha.2019.108951.
- [26] Bennett MR. In-stent stenosis: pathology and implications for the development of drug eluting stents. Heart (British Cardiac Society). 2003; 89: 218–224. https://doi.org/10.1136/heart.89. 2.218.
- [27] Yen WC, Fischer MM, Axelrod F, Bond C, Cain J, Cancilla B, et al. Targeting Notch signaling with a Notch2/Notch3 antagonist (tarextumab) inhibits tumor growth and decreases tumorinitiating cell frequency. Clinical Cancer Research: an Official Journal of the American Association for Cancer Research. 2015; 21: 2084–2095. https://doi.org/10.1158/1078-0432.CC R-14-2808.
- [28] Shi Q, Xue C, Zeng Y, Yuan X, Chu Q, Jiang S, et al. Notch signaling pathway in cancer: from mechanistic insights to targeted therapies. Signal Transduction and Targeted Therapy. 2024; 9: 128. https://doi.org/10.1038/s41392-024-01828-x.
- [29] Vu T, Jin L, Datta PK. Effect of Cigarette Smoking on Epithelial to Mesenchymal Transition (EMT) in Lung Cancer. Journal of Clinical Medicine. 2016; 5: 44. https://doi.org/10.3390/jcm5040044.
- [30] Tu W, Wang H, Li S, Liu Q, Sha H. The Anti-Inflammatory and Anti-Oxidant Mechanisms of the Keap1/Nrf2/ARE Signaling Pathway in Chronic Diseases. Aging and Disease. 2019; 10: 637–651. https://doi.org/10.14336/AD.2018.0513.
- [31] Hibdon ES, Razumilava N, Keeley TM, Wong G, Solanki S, Shah YM, et al. Notch and mTOR Signaling Pathways Promote Human Gastric Cancer Cell Proliferation. Neoplasia (New York, N.Y.). 2019; 21: 702–712. https://doi.org/10.1016/j.neo.2019.05.002.
- [32] Kang JH, Kawano T, Murata M, Toita R. Vascular calcification and cellular signaling pathways as potential therapeutic targets. Life Sciences. 2024; 336: 122309. https://doi.org/10.1016/j.lfs. 2023.122309.
- [33] Saxton RA, Sabatini DM. mTOR Signaling in Growth, Metabolism, and Disease. Cell. 2017; 168: 960–976. https://doi.org/10.1016/j.cell.2017.02.004.
- [34] Lin X, Li S, Wang YJ, Wang Y, Zhong JY, He JY, *et al.* Exosomal Notch3 from high glucose-stimulated endothelial cells regulates vascular smooth muscle cells calcification/aging. Life Sciences. 2019; 232: 116582. https://doi.org/10.1016/j.lfs.2019.116582.
- [35] Cui Y, Fang J, Guo H, Cui H, Deng J, Yu S, et al. Notch3-Mediated mTOR Signaling Pathway Is Involved in High

- Glucose-Induced Autophagy in Bovine Kidney Epithelial Cells. Molecules (Basel, Switzerland). 2022; 27: 3121. https://doi.org/10.3390/molecules27103121.
- [36] Cui Y, Guo H, Zhang Q, Fang J, Xie Y, Chen S, et al. The combination of high glucose and LPS induces autophagy in bovine kidney epithelial cells via the Notch3/mTOR signaling pathway. BMC Veterinary Research. 2022; 18: 307. https://doi.org/10.1186/s12917-022-03395-1.
- [37] Cao W, Li J, Yang K, Cao D. An overview of autophagy: Mechanism, regulation and research progress. Bulletin du Cancer. 2021; 108: 304–322. https://doi.org/10.1016/j.bulcan.2020.11. 004.
- [38] Mizushima N, Yoshimori T, Levine B. Methods in mammalian autophagy research. Cell. 2010; 140: 313–326. https://doi.org/ 10.1016/j.cell.2010.01.028.
- [39] Lamark T, Svenning S, Johansen T. Regulation of selective autophagy: the p62/SQSTM1 paradigm. Essays in Biochemistry. 2017; 61: 609–624. https://doi.org/10.1042/EBC20170035.
- [40] Santarino IB, Viegas MS, Domingues NS, Ribeiro AM, Soares MP, Vieira OV. Involvement of the p62/NRF2 signal transduction pathway on erythrophagocytosis. Scientific Reports. 2017; 7: 5812. https://doi.org/10.1038/s41598-017-05687-1.
- [41] Birgisdottir ÅB, Mouilleron S, Bhujabal Z, Wirth M, Sjøttem E, Evjen G, *et al.* Members of the autophagy class III phosphatidylinositol 3-kinase complex I interact with GABARAP and GABARAPL1 via LIR motifs. Autophagy. 2019; 15: 1333–1355. https://doi.org/10.1080/15548627.2019.1581009.
- [42] Menon MB, Dhamija S. Beclin 1 Phosphorylation at the Center of Autophagy Regulation. Frontiers in Cell and Developmental Biology. 2018; 6: 137. https://doi.org/10.3389/fcell.2018. 00137.
- [43] Qiu X, Xu Q, Xu T, Wan P, Sheng Z, Han Y, et al. Metformin alleviates β-glycerophosphate-induced calcification of vascular smooth muscle cells via AMPK/mTOR-activated autophagy. Experimental and Therapeutic Medicine. 2021; 21: 58. https://doi.org/10.3892/etm.2020.9490.
- [44] Tan P, Wang H, Zhan J, Ma X, Cui X, Wang Y, et al. Rapamycin induced miR 30a downregulation inhibits senescence of VSMCs by targeting Beclin1. International Journal of Molecular Medicine. 2019; 43: 1311–1320. https://doi.org/10.3892/ijmm.2019.4074.
- [45] Qu Y, Zhang N, Zhao Y. Resveratrol Inhibits Abdominal Aortic Aneurysm Progression by Reducing Extracellular Matrix Degradation, Apoptosis, Autophagy, and Inflammation of Vascular Smooth Muscle Cells via Upregulation of HMOX1. Journal of Endovascular Therapy: an Official Journal of the International Society of Endovascular Specialists. 2023; 15266028231202727. https://doi.org/10.1177/15266028231202727.
- [46] El-Tanani M, Nsairat H, Mishra V, Mishra Y, Aljabali AAA, Serrano-Aroca Á, et al. Ran GTPase and Its Importance in Cellular Signaling and Malignant Phenotype. International Journal of Molecular Sciences. 2023; 24: 3065. https://doi.org/10.3390/ ijms24043065.
- [47] Zhang MS, Arnaoutov A, Dasso M. RanBP1 governs spindle assembly by defining mitotic Ran-GTP production. Developmental Cell. 2014; 31: 393–404. https://doi.org/10.1016/j.devc el.2014.10.014.
- [48] Zolotukhin AS, Felber BK. Mutations in the nuclear export signal of human ran-binding protein RanBP1 block the Revmediated posttranscriptional regulation of human immunodeficiency virus type 1. The Journal of Biological Chemistry. 1997; 272: 11356–11360. https://doi.org/10.1074/jbc.272.17.11356.
- [49] Saxton RA, Sabatini DM. mTOR Signaling in Growth, Metabolism, and Disease. Cell. 2017; 169: 361–371. https://doi.org/10.1016/j.cell.2017.03.035.

